Emergent quantization from a dynamic vacuum

Harold White,* Jerry Vera, Andre Sylvester, and Leonard Dudzinski
Casimir, Inc., 16441 Space Center Boulevard, Bldg. D-200, Houston, Texas 77058, USA

(Received 24 October 2025; accepted 18 February 2026; published 9 March 2026)

We show that adding quadratic temporal dispersion to a dynamic-vacuum acoustic model yields a fully analytic, exactly isospectral mapping to the hydrogenic Coulomb problem. In the regime $\omega = Dq^2$ with $D = \hbar/(2m_{\text{eff}})$, a proton-imprinted constitutive profile produces an inverse sound speed $1/c_s^2(r) = A(\omega) + C(\omega)/r$ and hence a time-harmonic operator $(\nabla^2 + k_{\text{eff}}^2)$ that is Coulombic at each bound eigenfrequency. Separation of variables yields the exact hydrogenic eigenfunctions $R_{n\ell}(r)Y_\ell^m(\theta, \phi)$; the angular labels (ℓ, m) emerge naturally from the Laplace-Beltrami spectrum on $\mathbb{S}^2$ via rotational symmetry and boundary conditions (as in standard quantum mechanics), while localization follows from $A(\omega_n) < 0$ in a reactive stop band consistent with causal, passive dispersion. While angular-momentum quantization follows directly from rotational symmetry and boundary conditions in standard quantum mechanics (consistent with Noether's theorem), here it emerges within a classical-like dispersive acoustic framework without introducing additional wave-mechanical postulates beyond symmetry and self-adjointness. This highlights dispersion's role in bridging a hydrodynamic description to quantumlike spectral structure. Identifying $q_n \equiv \kappa_n$ maps spatial scale to frequency, giving $\omega_n = D\kappa_n^2 \propto 1/n^2$ and reproducing the Rydberg ladder. Calibration to the reduced-mass Rydberg frequency $(\omega_* = 2\pi cR_H)$ fixes $D = \hbar/(2\mu)$ and $m_{\text{eff}} = \mu$, with no free parameters. We determine the frequency dependence of $A(\omega_n)$ and $C(\omega_n)$ consistent with the underlying dispersive physics and demonstrate agreement with hydrogenic mode shapes and transition lines. The framework also predicts isotope shifts $[\mu \to \mu(M)]$ and symmetry-respecting Stark/Zeeman analogues. Dispersion thus renders quantization an emergent consequence of symmetry, boundary conditions, and causal response in a dynamic vacuum.

DOI: 10.1103/l8y7-r3rm

I. INTRODUCTION

In our prior work [1], we derived an acoustic wave equation from the Schrödinger equation via Madelung hydrodynamics and demonstrated numerically that hydrogenic orbital morphologies arise as acoustic resonances of a dynamic vacuum. The present work supplies the missing temporal-dispersion closure needed to make the mapping fully analytic and exactly isospectral to the hydrogenic Coulomb problem. The physical basis for this dispersion, rooted in linearized Madelung hydrodynamics, is derived in the Appendix.

(1) *Temporal dispersion of the medium*: Small longitudinal disturbances obey a quadratic dispersion in the regime of interest:

$$\omega = D\,q^2, \quad D = \frac{\hbar}{2\,m_{\text{eff}}}. \tag{1}$$

The dispersive closure is a quadratic law in the regime of interest (derived from Madelung hydrodynamics with quantum potential Q in the Appendix), which converts a spatial inverse length into an oscillation frequency. By itself, Eq. (1) does not quantize anything; it only maps scale to rate. This quadratic regime is the long-wavelength/quantum-pressure limit of the Madelung/Bogoliubov linearization [2] and also arises in gradient-elastic continua [3–6].

(2) *Spatial constitutive profile of the dynamic vacuum*: A proton-imprinted, radially varying medium $[\rho(r) = \gamma/r^4]$ and a finite far-field background make the local inverse sound speed

$$\frac{1}{c_s^2(r)} = A(\omega) + \frac{C(\omega)}{r}, \tag{2}$$

which makes the time-harmonic acoustic operator $(\nabla^2 + k_{\text{eff}}^2)$ *Coulombic*:

$$k_{\text{eff}}^2(r;\omega) = \frac{\omega^2}{c_s^2(r)} = \omega^2\left(A + \frac{C}{r}\right) \equiv \alpha(\omega) + \frac{\beta(\omega)}{r}. \tag{3}$$

Note. We distinguish (a) the plane-wave (spectral) wave number q appearing in the dispersion (1); (b) the spatial operator coefficient $k_{\text{eff}}(r;\omega)$ in Eq. (3); and (c) the bound-state inverse length $\kappa \equiv \sqrt{-\alpha}$ that characterizes the evanescent tail of a normalizable solution. In a uniform medium, k_{eff} would coincide with the spectral wave number, but here the inhomogeneity (the $1/r$ term) is what generates hydrogenic structure, so we keep these symbols distinct. We only *identify* $q_n \equiv \kappa_n$ when using the dispersion to map spatial scale to frequency.

The next steps complete the development of the full hydrogenic eigenfunctions and observed spectrum. With Eqs. (2)

*Contact author: sonny@casimirspace.com

Published by the American Physical Society under the terms of the Creative Commons Attribution 4.0 International license. Further distribution of this work must maintain attribution to the author(s) and the published article's title, journal citation, and DOI.

and (3), separation of variables $p = R_\ell(r)Y_\ell^m(\theta,\phi)$ yields the radial ordinary differential equation (ODE)

$$u''(r) + \left[\alpha(\omega) + \frac{\beta(\omega)}{r} - \frac{\ell(\ell+1)}{r^2}\right]u(r) = 0, \quad u = rR_\ell.$$

Choosing the (causal, dispersive) coefficients at the eigenfrequencies ω_n, one has $\alpha(\omega_n) = -\kappa_n^2$ and $\beta(\omega_n) = \beta$ (independent of n or a constant for all eigenfrequencies) makes this ODE *identical* to the hydrogenic Coulomb equation [7]. Regularity at $r = 0$ and decay as $r \to \infty$ (which requires $A(\omega_n) < 0$, i.e., a reactive stop band) then quantize the spatial scale and angular momentum:

$$\kappa_n = \frac{\beta}{2n}, \quad \ell = 0, 1, 2, \ldots, \quad m = -\ell, \ldots, \ell.$$

Thus, the full hydrogenic eigenfunctions $R_{n\ell}(r)Y_\ell^m(\theta,\phi)$ and the (n,ℓ,m) labels emerge from the spatial eigenproblem—they are not postulated.

Once the spatial quantization is established, the *temporal* dispersion (1) maps κ_n to eigenfrequencies by the identification $q_n \equiv \kappa_n$:

$$\omega_n = D\kappa_n^2 = D\frac{\beta^2}{4}\frac{1}{n^2} \implies E_n = -\hbar\,\omega_n \propto -\frac{1}{n^2}.$$

Calibrating $D = \hbar/(2\mu)$ (electron-proton reduced mass μ) aligns the dispersion constant with the kinetic-energy operator of the Schrödinger equation, while choosing $\beta = 2/a_0$ sets the effective coupling scale so that the resulting eigenvalues reproduce the Rydberg series. Here, $a_0 = 4\pi\varepsilon_0\hbar^2/(\mu e^2)$ is the Bohr radius, which thus enters only as a calibration scale rather than an assumed quantum postulate. Item (2) (the Coulombic operator) *creates* the quantized hydrogenic spatial spectrum and angular momentum; item (1) (the quadratic dispersion) *converts* each quantized spatial scale into the correct $1/n^2$ energy/frequency ladder. Together, they render the acoustic problem *isospectral* to hydrogen in both eigenfunctions and spectrum, with a single reduced-mass calibration (which simultaneously fixes the Bohr radius and energy scale) to observation. In short, once the dynamic vacuum is endowed with the quadratic dispersion of Eq. (1) and the Coulombic constitutive profile of Eq. (3), the acoustic Helmholtz problem becomes Coulombic, angular-momentum quantization *emerges* from symmetry, bound states follow from $A < 0$ [8], and the spectrum matches observation with a single reduced-mass calibration. The remainder of the paper develops this construction, details the frequency dependence of $A(\omega)$ and $C(\omega)$, and compares predicted levels and lines to hydrogen data.

II. MINIMAL ASSUMPTIONS AND DISPERSION

We make a compact set of explicit assumptions that together fix the governing operator, the spectrum, and the mapping to observation. No postulate of angular-momentum quantization is required.

(1) *Medium and governing equation*: The vacuum is modeled as a longitudinal, compressible continuum with spatially varying fields $\rho(\mathbf{r})$ (effective density) and $B(\mathbf{r})$ (bulk modulus). Small-signal dynamics (to leading order, lossless) obey

$$\nabla\cdot[\rho(\mathbf{r})^{-1}\nabla p] - B(\mathbf{r})^{-1}\,\partial_t^2 p = 0, \tag{4a}$$

$$(\nabla^2 + k_{\rm eff}^2)\,p = 0, \tag{4b}$$

$$k_{\rm eff}^2(\mathbf{r}) = \omega^2/c_s^2(\mathbf{r}), \tag{4c}$$

$$c_s^2 = B/\rho. \tag{4d}$$

(2) *Near-field density law (proton imprint)*: Guided by the electrostatic energy density around a proton, the near-field density scales as

$$\rho(r) = \frac{\gamma}{r^4}, \quad \gamma > 0 \text{ constant.} \tag{5}$$

(An ambient ρ_∞ is included without changing the conclusions below.)

(3) *Bulk modulus ansatz (Coulombic map)*: The effective inverse sound speed has a constant background plus a $1/r$ term,

$$\frac{1}{c_s^2(r)} = \frac{\rho(r)}{B(r)} = A(\omega) + \frac{C(\omega)}{r}, \tag{6}$$

realized, for example, by $B(r) = B_\infty + \beta_B/r^3$ together with Eq. (5) [9], giving $A = \rho_\infty/B_\infty$ (if $\rho_\infty \neq 0$) and $C = \gamma/\beta_B$. Consequently,

$$k_{\rm eff}^2(r) = \frac{\omega^2}{c_s^2(r)} = \omega^2\left(A + \frac{C}{r}\right) \equiv \alpha + \frac{\beta}{r}. \tag{7}$$

This is the *Coulombic* $(1/r)$ structure required for hydrogenic isospectrality.

(4) *Dispersion (linchpin)*: The longitudinal mode is dispersive with a quadratic (Schrödinger-like) law,

$$\omega = D\,q^2, \quad D = \frac{\hbar}{2\,m_{\rm eff}}. \tag{8}$$

The full linearized Madelung dispersion has the form $\omega^2 = c_L^2k^2 + D^2k^4$; a concise derivation is given in the Appendix, which connects the spatial inverse length q to temporal frequency. This form is the short-wavelength limit of the standard Bogoliubov relation $\omega^2 = c_s^2q^2 + (\hbar^2/4m_{\rm eff}^2)q^4$ [5], and also arises in gradient-elastic continua. It uniquely yields the observed $1/n^2$ spectrum once the spatial operator is Coulombic.

Notation: The plane-wave wave number q, the spatial operator coefficient $k_{\rm eff}(r;\omega)$, and the bound-state inverse length $\kappa = \sqrt{-\alpha}$ are kept distinct; only at discrete eigenfrequencies ω_n do we identify $q_n \equiv \kappa_n$ when mapping spatial scale to frequency.

(5) *Symmetry and boundary conditions*: Spherical symmetry applies for the single-proton problem. Solutions are regular at $r = 0$ and square integrable (evanescent) as $r \to \infty$. The latter requires

$$\lim_{r\to\infty} k^2(r) = \alpha = \omega^2 A(\omega) = -\kappa^2 < 0$$
$$\Rightarrow \quad A(\omega) < 0, \tag{9}$$

i.e., a reactive (stop-band) far field that produces the familiar exponential tails.

(6) *Observation mapping and calibration*: The dispersion maps each spatial eigenvalue κ_n to a temporal frequency by

$q_n \equiv \kappa_n$, giving

$$\omega_n = D\,\kappa_n^2 = D\,\frac{\beta^2}{4}\,\frac{1}{n^2}, \tag{10}$$

so that $E_n = -\hbar\,\omega_n \propto -1/n^2$. Calibration to hydrogen data uses the reduced-mass Rydberg constant R_H with $\omega_* = 2\pi c R_H$ and $\beta = 2/a_0$, yielding

$$D = \omega_* a_0^2 = \frac{\hbar}{2\,\mu}, \tag{11}$$

so the effective mass of the longitudinal mode equals the electron-proton reduced mass μ.

Results of assumptions. With Eq. (7), separation of $p = R_\ell(r) Y_\ell^m(\theta, \phi)$ and $u = rR_\ell$ gives

$$u''(r) + \left[\alpha + \frac{\beta}{r} - \frac{\ell(\ell+1)}{r^2}\right] u(r) = 0, \tag{12}$$

the hydrogenic Coulomb radial equation. Hence, the acoustic problem is *isospectral* to hydrogen: $\kappa = \sqrt{-\alpha}$, $n = \beta/(2\kappa) = n_r + \ell + 1$, and

$$R_{n\ell}(r) \propto (2\kappa r)^\ell e^{-\kappa r} L_{n-\ell-1}^{(2\ell+1)}(2\kappa r), \tag{13a}$$

$$p_{n\ell m} \propto R_{n\ell}(r)\, Y_\ell^m(\theta, \phi). \tag{13b}$$

Quantization of ℓ and m emerges naturally from spherical symmetry; it is not an added axiom. Once the medium is endowed with the quadratic dispersion of Eq. (8) and the Coulombic constitutive profile of Eq. (7), the dynamic-vacuum acoustic problem reproduces the hydrogenic spectrum and eigenfunctions, with a single reduced-mass calibration to observation.

Operator matching and self-adjointness. The time-harmonic equation $(\nabla^2 + k_{\text{eff}}^2)p = 0$ with $k_{\text{eff}}^2(r) = \omega^2(A + C/r)$ separates in spherical coordinates. Writing $p(r, \theta, \phi) = R_\ell(r) Y_\ell^m(\theta, \phi)$ and $u = rR_\ell$ gives [10]

$$u''(r) + \left[\alpha(\omega) + \frac{\beta(\omega)}{r} - \frac{\ell(\ell+1)}{r^2}\right] u(r) = 0,$$
$$u(0) = u(\infty) = 0.$$

Comparing with the Coulomb Schrödinger equation $u'' + [2\mu E/\hbar^2 + (2\mu e^2/4\pi\varepsilon_0\hbar^2)(1/r) - \ell(\ell+1)/r^2]u = 0$ identifies

$$\alpha(\omega) = \frac{2\mu E}{\hbar^2}, \quad \beta(\omega) = \frac{2\mu e^2}{4\pi\varepsilon_0\hbar^2} \equiv \beta,$$

showing that the acoustic operator is mathematically identical to the hydrogenic Coulomb operator. For bound states $E < 0$, $\alpha(\omega_n) = -\kappa_n^2$ with $\kappa_n = \beta/(2n)$. The normalized radial functions are

$$R_{n\ell}(r) = \mathcal{N}_{n\ell}(2\kappa_n r)^\ell e^{-\kappa_n r} L_{n-\ell-1}^{(2\ell+1)}(2\kappa_n r),$$
$$\mathcal{N}_{n\ell} = (2\kappa_n)^{3/2}\sqrt{\frac{(n-\ell-1)!}{2n(n+\ell)!}}.$$

These eigenfunctions form a complete orthonormal basis for each ℓ and confirm the exact isospectrality between the dynamic-vacuum acoustic operator and hydrogenic quantum mechanics.

III. EMERGENT ANGULAR MOMENTUM FROM SPHERICAL SYMMETRY

In this construction, the angular quantum numbers are *not* postulated. They emerge from the spherical symmetry of the single-proton problem, the scalar character of the acoustic pressure p, and the requirement of regularity and single-valuedness on the compact angular manifold $\mathbb{S}^2$. For any central constitutive profile $k_{\text{eff}}^2(r; \omega)$, the Laplacian separates as

$$\nabla^2 = \frac{1}{r^2}\,\partial_r(r^2\partial_r) - \frac{\hat{L}^2}{r^2},$$
$$\hat{L}^2 = -\left[\frac{1}{\sin\theta}\,\partial_\theta(\sin\theta\,\partial_\theta) + \frac{1}{\sin^2\theta}\,\partial_\phi^2\right]. \tag{14}$$

Substituting $p(r, \theta, \phi) = R(r)Y(\theta, \phi)$ into $(\nabla^2 + k_{\text{eff}}^2)p = 0$ gives the separated equations

$$\hat{L}^2 Y = \lambda Y, \quad \frac{1}{r^2}\partial_r(r^2\partial_r R) + \left[k_{\text{eff}}^2(r; \omega) - \frac{\lambda}{r^2}\right] R = 0. \tag{15}$$

On the compact sphere $\mathbb{S}^2$, the conditions of single-valuedness in ϕ (2π-periodicity) and regularity at the poles $\theta = 0, \pi$ enforce the discrete Laplace-Beltrami spectrum

$$\lambda = \ell(\ell+1),$$
$$\ell = 0, 1, 2, \ldots,$$
$$m = -\ell, \ldots, \ell, \tag{16}$$

with orthonormal eigenfunctions $Y_\ell^m(\theta, \phi)$ [11,13]. Thus, the integer labels ℓ, m are an *emergent spectral property* of the angular eigenproblem on $\mathbb{S}^2$, not an additional quantization axiom.

Defining $u(r) \equiv r\,R(r)$ removes the first derivative from the radial equation:

$$u''(r) + \left[k_{\text{eff}}^2(r; \omega) - \frac{\ell(\ell+1)}{r^2}\right] u(r) = 0, \quad u(0) = 0,$$
$$u(\infty) = 0. \tag{17}$$

For the Coulombic constitutive map $k_{\text{eff}}^2(r; \omega) = \alpha(\omega) + \beta(\omega)/r$ (Sec. II), Eq. (17) becomes the hydrogenic radial ODE. Normalizability enforces the usual Laguerre solutions $R_{n\ell}(r)$ with $n = n_r + \ell + 1$ and the familiar degeneracies: For each n, the allowed ℓ are $0, 1, \ldots, n-1$, and each ℓ supports a $(2\ell + 1)$-fold magnetic degeneracy in m (total n^2).

Takeaway. Discrete angular momentum arises automatically from the symmetry of the problem—The Laplace-Beltrami spectrum on $\mathbb{S}^2$ and the scalar nature of p are sufficient. The centrifugal term $\ell(\ell+1)/r^2$ and the hydrogenic degeneracies follow without any extra quantization postulate.

IV. MAPPING TO OBSERVATION, DISPERSIVE PARAMETERS, AND VALIDATION

The spatial eigenproblem fixes the bound-state scale and eigenfunctions,

$$\kappa_n = \frac{1}{n\,a_0}, \quad p_{n\ell m}(r, \theta, \phi) = A_{n\ell m}\,R_{n\ell}(r)\,Y_\ell^m(\theta, \phi), \tag{18}$$

TABLE I. Energylike level values using reduced mass consistently (R_H). Both analytic and observation columns use R_H. Frequencies in PHz. Constants from CODATA 2018 [14].

n	$\|E_n\|$ analytic (eV)	f_n analytic (PHz)	$\|E_n\|$ obs (eV)	f_n obs (PHz)
1	13.598 434 006	3.288 051	13.598 434 006	3.288 051
2	3.399 608 501	0.822 013	3.399 608 501	0.822 013
3	1.510 937 112	0.365 339	1.510 937 112	0.365 339
4	0.849 902 125	0.205 503	0.849 902 125	0.205 503
5	0.543 937 360	0.131 522	0.543 937 360	0.131 522
6	0.377 734 278	0.091 335	0.377 734 278	0.091 335
7	0.277 518 041	0.067 103	0.277 518 041	0.067 103

so the quantized inverse length directly determines each level's frequency via the quadratic dispersion relation,

$$\omega_n = D\,\kappa_n^2 = \frac{\omega_*}{n^2}, \quad E_n = -\hbar\,\omega_n \propto -\frac{1}{n^2}. \tag{19}$$

The level differences reproduce the Rydberg ladder,

$$f_{n_2\to n_1} = \frac{\Delta E}{h} = \frac{\omega_*}{2\pi}\left(\frac{1}{n_1^2} - \frac{1}{n_2^2}\right) = c\,R_H\left(\frac{1}{n_1^2} - \frac{1}{n_2^2}\right), \tag{20}$$

with calibration $\omega_* = 2\pi c R_H$ using the reduced-mass Rydberg constant R_H [14].

Reduced-mass calibration. The electron-proton system uses $\mu = m_e m_p/(m_e + m_p) \approx 0.999\,46\,m_e$, which rescales the Bohr radius and Rydberg constant as

$$a_0^{(H)} = \frac{4\pi\varepsilon_0\hbar^2}{\mu e^2} = \frac{m_e}{\mu}\,a_0^{(\infty)}, \quad R_H = R_\infty\,\frac{\mu}{m_e}.$$

With $D = \omega_*(a_0^{(H)})^2$, one obtains

$$D = \frac{\hbar}{2\,\mu}, \quad m_{\rm eff} = \mu\,, \tag{21}$$

so the effective inertial parameter of the longitudinal mode equals the reduced mass. No further tuning is required: all absolute numbers follow from R_H and $a_0^{(H)}$.

Frequency-dependent parameters. From $k_{\rm eff}^2 = \omega^2(A + C/r) = \alpha + \beta/r$, $\alpha_n = -1/(n^2 a_0^2)$, and $\beta = 2/a_0$, the dispersion-linked coefficients are

$$A(\omega_n) = -\frac{n^2}{a_0^2\,\omega_*^2}, \quad C(\omega_n) = \frac{2n^4}{a_0\,\omega_*^2}. \tag{22}$$

Hence, $A < 0$ identifies a reactive (stop-band) far field where modes are evanescent and localized, while $C > 0$ represents the proton-induced increase of $1/c_s^2$ near the core. Their monotonic scalings $|A| \propto n^2$, $C \propto n^4$ reflect how different eigenfrequencies probe different points of the same dispersive response function.

Material interpretation. Using $\rho(r) = \gamma/r^4$ and $B(r) = B_\infty + \beta_B/r^3$, one has $1/c_s^2 = \rho/B \simeq A + C/r$ with $A = \rho_\infty/B_\infty$ and $C = \gamma/\beta_B$, so

$$B_\infty(\omega_n) = -\,\rho_\infty\,\frac{a_0^2\omega_*^2}{n^2}, \quad \beta_B(\omega_n) = \gamma\,\frac{a_0\omega_*^2}{2n^4}.$$

Both scale inversely with powers of n, consistent with the frequency-dependent elasticity needed to maintain Coulombic isospectrality.

Validation. Once the dispersion and reduced-mass calibration are fixed, the framework has *no free parameters*. The eigenfunctions are hydrogenic and the levels follow the $1/n^2$ law. Tables I and II compare analytic and observed hydrogen data (identical within precision), and Fig. 1 visualizes selected isosurfaces of $|\psi_{n\ell m}|^2$. The spatial morphology and transition

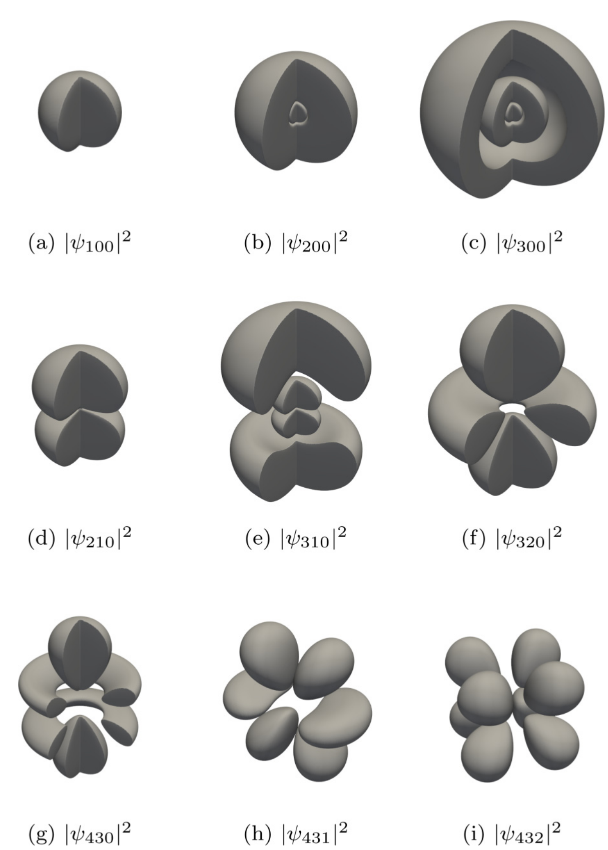

FIG. 1. Hydrogenic orbital density isosurfaces: Each panel shows the isosurface of the analytic probability density $|\psi_{n\ell m}(x,y,z)|^2$ at a fixed physical threshold (nm^{-3}), computed from $R_{n\ell}(r)$ and real $Y_\ell^m(\theta,\phi)$. Isosurfaces were extracted via a marching-cubes method; a narrow angular "pie-wedge" was masked in volume prior to extraction to reveal interior structure, and gray shading is illustrative only. These visualizations match the familiar textbook morphology of hydrogenic orbitals [11].

TABLE II. Selected hydrogen vacuum lines using reduced mass consistently (R_H). Both analytic and observation columns use R_H. Frequencies in PHz and wavelengths in nm. Constants from CODATA 2018 [14]; observed values cross-checked with NIST ASD [15].

Transition	f analytic (PHz)	λ analytic (nm)	f obs (PHz)	λ obs (nm)
Lyman-α ($2 \to 1$)	2.466 038	121.568 446	2.466 038	121.568 446
Lyman-β ($3 \to 1$)	2.922 712	102.573 376	2.922 712	102.573 376
Lyman-γ ($4 \to 1$)	3.082 576	97.087 384	3.082 576	97.087 384
Hα ($3 \to 2$)	0.456 674	656.281 106	0.456 674	656.281 106
Hβ ($4 \to 2$)	0.609 285	492.162 878	0.609 285	492.162 878
Balmer-γ ($5 \to 2$)	0.654 573	456.867 793	0.654 573	456.867 793
Paschen-α ($4 \to 3$)	0.159 836	1 875.627 447	0.159 836	1 875.627 447
Paschen-β ($5 \to 3$)	0.233 817	1 282.167 200	0.233 817	1 282.167 200

frequencies match hydrogen exactly, demonstrating that the dynamic-vacuum construction reproduces the observed Rydberg spectrum with a single reduced-mass calibration.

V. DISCUSSION AND CONCLUSION

Quadratic dispersion, $\omega = Dq^2$ with $D = \hbar/(2m_{\text{eff}})$, is the essential ingredient that renders the dynamic-vacuum acoustic problem analytically isospectral with hydrogen. With the minimal constitutive map $1/c_s^2(r) = A(\omega) + C(\omega)/r$ and near-field density $\rho(r) = \gamma/r^4$, the time-harmonic operator $(\nabla^2 + k_{\text{eff}}^2)$ becomes exactly Coulombic. Separation then produces the standard hydrogenic basis $R_{n\ell}(r)Y_\ell^m(\theta, \phi)$; angular-momentum quantization arises naturally from the $\mathbb{S}^2$ eigenproblem, and localization follows from $A(\omega_n) < 0$.

Calibration to observation through the reduced-mass Rydberg frequency $\omega_* = 2\pi c R_H$ fixes all constants and implies $D = \hbar/(2\mu)$, with $m_{\text{eff}} = \mu$ (the electron-proton reduced mass). Without additional parameters, the model reproduces the hydrogenic shapes (Fig. 1), the $1/n^2$ level spacing and Rydberg ladder (Tables I and II), and isotope shifts via $\mu \to \mu(M)$. Weak, slowly varying perturbations of $1/c_s^2(\mathbf{r})$ introduce Stark- or Zeeman-type splittings on the same analytic basis, confirming the robustness of the mapping.

This framework parallels the hydrodynamic or Madelung formulation, where dispersion enters as a quantumlike correction. Here, however, the quadratic regime alone suffices to produce full isospectrality, revealing quantization as an emergent property of a dispersive, dynamic vacuum rather than an imposed axiom. Subleading corrections ($O(1/r^2)$) or small loss terms would shift line centers or set linewidths perturbatively but do not alter the analytic core. Extensions to multicenter or externally forced problems follow from the same separation principles.

In summary, a single physically motivated assumption—quadratic dispersion—yields a closed, analytic, and observationally calibrated construction of the hydrogen spectrum. Angular momentum emerges from geometry, bound states from $A < 0$, and the spectral ladder from one reduced-mass calibration. The result is a self-consistent, dispersion-anchored dynamic-vacuum model in which quantization arises naturally from the symmetry of the medium itself.

ACKNOWLEDGMENTS

The authors thank Casimir for institutional support during the development of the analytic model. Special thanks to R. Efraim and D. Narea for helpful comments on manuscript readability. AI tools were used to assist with enhancing readability and communicating ideas.

DATA AVAILABILITY

No data were created or analyzed in this study.

APPENDIX: DISPERSION RELATION FROM MADELUNG HYDRODYNAMICS WITH QUANTUM POTENTIAL

1. Starting point: Schrödinger equation

Consider a nonrelativistic scalar field of effective mass μ governed by the Schrödinger equation

$$i\hbar \frac{\partial \psi}{\partial t} = -\frac{\hbar^2}{2\mu}\nabla^2\psi + V(\mathbf{x})\psi, \tag{A1}$$

where $V(\mathbf{x})$ is an external or mean-field potential. We perform the Madelung transformation

$$\psi(\mathbf{x}, t) = \sqrt{\rho(\mathbf{x}, t)}\, e^{iS(\mathbf{x},t)/\hbar} \tag{A2}$$

and define the hydrodynamic velocity field

$$\mathbf{v} = \frac{\nabla S}{\mu}. \tag{A3}$$

2. Madelung hydrodynamic equations

Substituting into Eq. (A1) and separating real and imaginary parts yields the continuity equation

$$\frac{\partial \rho}{\partial t} + \nabla \cdot (\rho \mathbf{v}) = 0, \tag{A4}$$

and an Euler-like momentum equation,

$$\mu\left(\frac{\partial \mathbf{v}}{\partial t} + (\mathbf{v}\cdot\nabla)\mathbf{v}\right) = -\nabla(V + Q), \tag{A5}$$

where the quantum potential Q is

$$Q(\mathbf{x}, t) = -\frac{\hbar^2}{2\mu}\frac{\nabla^2\sqrt{\rho}}{\sqrt{\rho}}. \tag{A6}$$

Consider the force/momentum equation (A5) in the case of static equilibrium (i.e., no acoustic excitation). In this scenario, the classical potential term ∇V represents the equilibrium pressure gradient $1/\rho_0 \nabla P_0$ of the vacuum. Under this equilibrium identification, the momentum equation (A5) may be expressed as

$$\mu\left(\frac{\partial \mathbf{v}}{\partial t} + (\mathbf{v}\cdot\nabla)\mathbf{v}\right) = -\frac{1}{\rho}\nabla P(\rho) - \nabla Q. \tag{A7}$$

In the presence of acoustic excitation, the classical potential contributes only through the background pressure profile, while the quantum potential governs the dynamical restoring force associated with density fluctuations.

3. Linearized equations for perturbations

We now consider small longitudinal perturbations about this equilibrium configuration:

$$\rho(\mathbf{x},t) = \rho_0 + \rho_1(\mathbf{x},t), \quad \mathbf{v}(\mathbf{x},t) = \mathbf{v}_1(\mathbf{x},t), \quad \rho_1 \ll \rho_0. \tag{A8}$$

We linearize about a static equilibrium state ($\rho_0, \mathbf{v}_0 = \mathbf{0}$) with a time-independent background potential. The following equations describe the dynamics of small perturbations about this state; any purely background force balance is absorbed into the equilibrium configuration.

From Eq. (A4), one obtains

$$\frac{\partial \rho_1}{\partial t} + \rho_0 \nabla\cdot\mathbf{v}_1 = 0. \tag{A9}$$

Assuming a barotropic equation of state $P = P(\rho)$, we expand about ρ_0:

$$P(\rho) \approx P(\rho_0) + \left.\frac{dP}{d\rho}\right|_{\rho_0}\rho_1. \tag{A10}$$

Defining the longitudinal sound speed

$$c_L^2 \equiv \frac{1}{\mu}\left.\frac{dP}{d\rho}\right|_{\rho_0}, \tag{A11}$$

the linearized pressure gradient becomes

$$-\frac{1}{\rho}\nabla P(\rho) \approx -\frac{\mu c_L^2}{\rho_0}\nabla\rho_1. \tag{A12}$$

a. Linearized quantum potential

Expanding the quantum potential (A6) to linear order in ρ_1 yields

$$Q \approx -\frac{\hbar^2}{4\mu\rho_0}\nabla^2\rho_1, \tag{A13}$$

so that

$$-\nabla Q \approx \frac{\hbar^2}{4\mu\rho_0}\nabla(\nabla^2\rho_1). \tag{A14}$$

b. Linearized momentum equation

For small-amplitude perturbations, the convective term $(\mathbf{v}\cdot\nabla)\mathbf{v}$ is second order in small quantities and can be neglected compared to the time derivative $\partial\mathbf{v}_1/\partial t$, i.e., $|(\mathbf{v}\cdot\nabla)\mathbf{v}| \ll |\partial\mathbf{v}/\partial t|$. The linearized form of Eq. (A7) is therefore

$$\mu\frac{\partial \mathbf{v}_1}{\partial t} = -\frac{\mu c_L^2}{\rho_0}\nabla\rho_1 + \frac{\hbar^2}{4\mu\rho_0}\nabla(\nabla^2\rho_1). \tag{A15}$$

4. Wave equation for density perturbations

Taking the divergence of Eq. (A15) gives

$$\mu\frac{\partial}{\partial t}(\nabla\cdot\mathbf{v}_1) = -\frac{\mu c_L^2}{\rho_0}\nabla^2\rho_1 + \frac{\hbar^2}{4\mu\rho_0}\nabla^4\rho_1. \tag{A16}$$

Using Eq. (A9) to eliminate $\nabla\cdot\mathbf{v}_1$, one obtains

$$\frac{\partial^2\rho_1}{\partial t^2} = c_L^2\nabla^2\rho_1 - \frac{\hbar^2}{4\mu^2}\nabla^4\rho_1. \tag{A17}$$

Equation (A17) is the linearized wave equation governing density perturbations in the Madelung fluid, including the contribution of the quantum potential.

5. Dispersion relation

Assuming a plane-wave solution

$$\rho_1(\mathbf{x},t) = \hat{\rho}\, e^{i(\mathbf{k}\cdot\mathbf{x}-\omega t)}, \tag{A18}$$

substitution into Eq. (A17) yields

$$\omega^2 = c_L^2 k^2 + \frac{\hbar^2}{4\mu^2}k^4. \tag{A19}$$

Defining

$$D \equiv \frac{\hbar}{2\mu}, \tag{A20}$$

the dispersion relation may be written compactly as

$$\boxed{\omega^2 = c_L^2 k^2 + D^2 k^4.} \tag{A21}$$

This dispersion relation contains both the acoustic (k^2) and quantum-pressure (k^4) contributions and follows directly from the Madelung hydrodynamic formulation when perturbations about a force-balanced vacuum background are considered.

[1] H. White, J. Vera, P. Bailey, P. March, T. Lawrence, A. Sylvester, and D. Brady, Acoustic derivation from Schrödinger and numerical evidence for orbital resonances in a dynamic vacuum, Phys. Open **1**, 100009 (2019).

[2] The Madelung/Bogoliubov linearization refers to expressing the Schrödinger or Gross-Pitaevskii equation in hydrodynamic form (via Madelung's transformation) and then linearizing about a uniform background density to obtain small-amplitude wave equations. This procedure yields the Bogoliubov dispersion relation $\omega^2 = c_s^2k^2 + \hbar^2k^4/4m^2$, where the first term corresponds to acoustic (phononlike) behavior and the second term arises from quantum-pressure effects. At low k (long wavelengths), the first term dominates and gives acoustic behavior ($\omega \propto k$); at high k (short wavelengths or quantum-pressure-

dominated regime), the second term dominates, yielding a quadratic dependence $\omega \propto k^2$.

[3] E. Madelung, Quantentheorie in hydrodynamischer form, Z. Phys. **40**, 322 (1927).

[4] N. N. Bogoliubov, On the theory of superfluidity, J. Phys. (USSR) **11**, 23 (1947).

[5] L. Pitaevskii and S. Stringari, *Bose-Einstein Condensation and Superfluidity* (Oxford University Press, Oxford, 2016), Chaps. 2 and 3.

[6] R. D. Mindlin, Micro-structure in linear elasticity, Arch. Rational Mech. Anal. **16**, 51 (1964).

[7] In this construction, the coefficients $\alpha(\omega)$ and $\beta(\omega)$ represent the effective response of the dispersive medium, analogous to the energy and Coulomb coupling terms in the hydrogenic Schrödinger equation. Because the medium is causal and frequency dependent, these coefficients vary with ω; however, the physically relevant solutions occur only at discrete eigenfrequencies ω_n. Evaluating the coefficients at these eigenfrequencies and imposing $\alpha(\omega_n) = -\kappa_n^2$ ensures that the effective propagation constant is imaginary, corresponding to a bound (evanescent) spatial mode. Setting $\beta(\omega_n) = \beta$, independent of n, keeps the $1/r$ coupling strength constant across all eigenstates. With these assignments, the radial equation reduces to the hydrogenic Coulomb equation. Thus, the quantized hydrogenic structure emerges naturally from the dispersive acoustic formulation without introducing it as an external assumption.

[8] The condition $A(\omega) < 0$ designates a reactive regime of the dispersive medium in which the effective squared wave number becomes negative, producing evanescent (spatially decaying) solutions rather than propagating waves. Physically, this corresponds to a stop band in which the stored reactive energy exceeds the kinetic component, confining the mode and creating a discrete bound state. In this sense, $A < 0$ plays the same role as negative total energy $E < 0$ in the Schrödinger formulation of hydrogen, marking the transition from continuum to bound eigenmodes.

[9] With $\rho(r) = \gamma/r^4$ and $B(r) = \beta_B/r^3$, one has $\rho/B = (\gamma/\beta_B)\, r^{-1}$ exactly; including a background B_∞ preserves the Coulombic $1/r$ core for $r \ll (\beta_B/B_\infty)^{1/3}$ while allowing a tunable constant term $A(\omega) = \rho_\infty(\omega)/B_\infty(\omega)$.

[10] With domain $u \in L^2((0, \infty), dr)$, the radial operator is self-adjoint, ensuring a real, discrete spectrum (Sturm-Liouville theory [12]).

[11] D. J. Griffiths and D. F. Schroeter, *Introduction to Quantum Mechanics*, 3rd ed. (Cambridge University Press, Cambridge, 2018).

[12] A. Zettl, *Sturm-Liouville Theory* (American Mathematical Society, Providence, 2005).

[13] G. B. Arfken, H. J. Weber, and F. E. Harris, *Mathematical Methods for Physicists*, 7th ed. (Academic Press, Oxford, 2013).

[14] E. Tiesinga, P. J. Mohr, D. B. Newell, and B. N. Taylor, CODATA recommended values of the fundamental physical constants: 2018, Rev. Mod. Phys. **93**, 025010 (2021).

[15] A. Kramida, Y. Ralchenko, J. Reader, and NIST ASD team, NIST atomic spectra database, version 5.x, https://physics.nist.gov/asd.